

Spin waves and phase diagram of one-dimensional, dipolar antiferromagnets

M. Hummel, C. Pich,* and F. Schwabl

Institut für Theoretische Physik, Physik-Department der Technischen Universität München, James-Franck-Strasse, 85747 Garching, Germany

(October 5, 2018)

We report on the properties of a dipolar, antiferromagnetic chain in the framework of linear spin-wave theory. As a model we use an isotropic Heisenberg-Hamiltonian with antiferromagnetic nearest neighbor exchange and anisotropic dipole-dipole interaction. The phase diagram is calculated for an arbitrary ratio of dipolar interaction to exchange interaction and for fields both parallel and perpendicular to the chain direction. We can distinguish two regions, an antiferromagnetic exchange dominated region, in which the dipole energy acts as a planar anisotropy and a ferromagnetic dipole dominated region, in which the dipole energy acts as an easy-axis anisotropy. The anisotropy in the field dependent magnetization, which is caused by quantum fluctuations, is several orders of magnitude larger than the anisotropy predicted by the classical theory. We show that the dipole-dipole interaction does not lead to long-range order in the pure one-dimensional case, however for quasi one-dimensional systems spin-waves are important. The calculated magnetization is compared with experimental measurements for RbMnBr_3 , a quasi one-dimensional antiferromagnet.

75.10.Jm, 75.30.Ds, 75.30.Gw, 75.50.Ee

*Present address: Physics Department, University of California, Santa Cruz, CA 95064.

I. INTRODUCTION

Low-dimensional magnetic systems have long attracted the attention of experimental and theoretical physics. In systems with reduced dimensionality the fluctuations are enhanced and can prevent a system from long-range ordering. For one- and two-dimensional isotropic Heisenberg ferro- and antiferromagnets with short-range interaction it has been proven exactly^{1,2} that long-range order is absent for finite temperatures. The existence of long-range order in low-dimensional systems depends crucially on anisotropies and long-range interactions, as there are single-ion anisotropy or the dipole-dipole interaction.

In real systems the dipole-dipole interaction is always present in addition to the short-range exchange interaction. Although the dipole-dipole energy is weak compared to the exchange energy it plays an important role in low-dimensional systems due to its anisotropic and long-range character. Maleev³ showed that in a two-dimensional ferromagnetic system the additional dipolar interaction leads to a modification of the spin-wave frequency in the long wavelength limit from a quadratic to a square root wave vector dependence, for which long-range order is established. For the antiferromagnetic counterpart on a square and a honeycomb lattice it has also been shown⁴ that dipolar interaction stabilizes long-range magnetic order at finite temperatures. In these cases, however, the dipolar anisotropy leads to a discrete ground state with spins oriented perpendicular to the plane, producing an energy gap in the dispersion relation. The finite Néel temperatures in various quasi two-dimensional systems (e.g. K_2MnF_4) have been calculated within the dipolar model⁴, in good agreement with the experimental values.

In recent papers⁵ we determined the magnetic phase diagram of the two-dimensional, dipolar Heisenberg antiferromagnet (square and honeycomb lattice) for fields along the easy-axis, i.e. perpendicular to the plane. In contrast to models with single-ion anisotropy or an anisotropic exchange interaction, we found that the dipole-dipole interaction establishes a new phase, an intermediate phase. With increasing field strength the system changes by second-order transitions from the Néel phase to an intermediate phase, a spin-flop phase and finally to a paramagnetic phase at high magnetic fields.

From the results in two dimensions we anticipate that also in quasi one-dimensional Heisenberg antiferromagnets, the dipolar interaction will reduce thermal and quantum fluctuations and thus increase the tendency to order.

In this paper we investigate the influence of the dipolar interaction on the classical ground states and on quantum fluctuations. It is shown that due to the competition of the exchange and dipolar interaction we can distinguish two regions, namely an exchange dominated and a dipolar dominated region. In the former the dipolar energy leads to a planar anisotropy, whereas in the lat-

ter it leads to an easy-axis anisotropy. We study the dispersion relations for various relative strengths of the dipolar interaction. In the exchange dominated region, the dipolar interaction breaks the continuous symmetry of the ground state partially and favors states with spins perpendicular to the chain direction. Rotation symmetry around the chain direction still exists. The dispersion relation for this phase is modified by the dipolar interaction, but as in the isotropic counterpart no long-range order can exist even for $T = 0$.

The most famous quasi one-dimensional systems are the ternary compounds ABX_3 (A alkaline, B transition metal and X halogen), which have been studied intensively experimentally in the context of Haldane's phase⁶ and solitonic excitations⁷. Of particular interest are the Mn compounds. Because the angular momentum L is zero, no crystal field splitting occurs in these systems and the dipole-dipole interaction should be the most important anisotropy. Experiments⁸ show an anisotropy in the magnetization measurements for fields applied parallel and perpendicular to the spin-chain axis. We will show that this anisotropy can be understood qualitatively by our simple one-dimensional dipolar model. Up to now, only partial aspects of the dipole-dipole interaction have been considered^{9,10}. In Ref[9] the classical ground state has been determined, but no excitations have been investigated, whereas in Ref[10] the dipolar interaction is only considered for nearest neighbors. In this paper the effects of the additional dipolar interaction will be studied in a systematic way.

In this spin wave theory we disregard kink-like excitations, which even for the r^{-3} decay of the dipolar interaction destroy one-dimensional long-range order. However, for wavelengths shorter than the correlation length magnon excitations become important. This has been shown experimentally by Steiner for CsNiF_3 ¹¹. The short range antiferromagnetic order supports spin waves with wave vectors not too close to the center of the Brillouin zone. Especially for quasi one-dimensional systems the weak interchain interaction leads to a stabilization of the magnetic order and spin waves become the relevant excitations.

The outline of this paper is as follows: in section II we introduce the dipolar model; in III we investigate the ground state, the spin-wave spectrum and the order parameter for vanishing fields; in IV we study the magnetic phase diagram for the whole parameter region. In the last section we apply our model to a quasi one-dimensional system, namely RbMnBr_3 .

II. MODEL

The Hamiltonian of a dipolar antiferromagnet reads

$$H = - \sum_{l \neq l'} \sum_{\alpha\beta} (J_{ll'} \delta_{\alpha\beta} + A_{ll'}^{\alpha\beta}) S_l^\alpha S_{l'}^\beta - g\mu_B \mathbf{H}_0 \sum_l \mathbf{S}_l, \quad (2.1)$$

with spins \mathbf{S}_l at lattice sites \mathbf{x}_l . The first term in brackets is the isotropic exchange interaction $J_{ll'}$ and the second term is the classical dipole-dipole-interaction

$$A_{ll'}^{\alpha\beta} = -\frac{1}{2}(g\mu_B)^2 \left(\frac{\delta_{\alpha\beta}}{|\mathbf{x}_l - \mathbf{x}_{l'}|^3} - \frac{3(\mathbf{x}_l - \mathbf{x}_{l'})_\alpha (\mathbf{x}_l - \mathbf{x}_{l'})_\beta}{|\mathbf{x}_l - \mathbf{x}_{l'}|^5} \right). \quad (2.2)$$

The third term in Eq. (2.1) describes the effect of an external magnetic field \mathbf{H}_0 , where g is the Landé-factor and μ_B is the Bohr magneton. From this Hamiltonian we calculate the magnon spectrum in the framework of the Holstein-Primakoff (HP)¹² transformation. The Holstein-Primakoff transformation is an exact transformation which expresses the Hamiltonian of Eq. (2.1) in terms of Bose operators a_l^\dagger, a_l . For low temperatures an expansion up to bilinear terms can be used

$$\tilde{S}_l^x = \sqrt{\frac{S}{2}}(a_l + a_l^\dagger), \quad \tilde{S}_l^y = -i\sqrt{\frac{S}{2}}(a_l - a_l^\dagger), \quad (2.3)$$

$$\tilde{S}_l^z = S - a_l^\dagger a_l.$$

The tilde indicates that we have to use these inner spin coordinates in the rotated coordinate frame where the z -direction lies in the direction of the classical spins. For the following discussion we define a dimensionless parameter κ , which gives the ratio between the dipolar energy and the exchange energy:

$$\kappa = \frac{(g\mu_B)^2}{c^3 J}. \quad (2.4)$$

Here J denotes the strength of the exchange energy (the negative sign of the antiferromagnetic exchange interaction $J_{ll'}$ is taken into account separately) and c denotes the distance between magnetic ions.

In the following we consider a spin chain which is directed along the x -axis (see Fig. 1a,b).

III. DIPOLAR ANTIFERROMAGNETIC CHAIN WITHOUT FIELD

The long-range dipole-dipole interaction and the antiferromagnetic exchange interaction compete with each other: while the latter favors an antiferromagnetic spin configuration, the former favors a ferromagnetic orientation along the chain axis. Thus, we can distinguish an exchange-dominated region and a dipole-dominated region, which are separated by the condition (to be shown in Eq. (3.19))

$$J_{\mathbf{q}_0} - J_0 + A_{\mathbf{q}_0}^{33} - A_0^{11} \leq 0, \quad (3.1)$$

where $J_{\mathbf{q}}$ is the Fourier transform of the exchange interaction $J_{ll'}$, which equals $J_{\mathbf{q}} = -2J \cos(q_x c)$ for nearest-neighbor interaction (in the following we set $q_x = q$), and $A_{\mathbf{q}}^{\alpha\beta}$ is the Fourier transform of the dipolar tensor Eq. (2.2)

$$A_{\mathbf{q}}^{\alpha\beta} = \sum_{l \neq 0} A_{l0}^{\alpha\beta} \exp(i\mathbf{q}\mathbf{x}_l), \quad (3.2)$$

which can be evaluated by Ewald summation¹³ (see appendix A). The wave vector $\mathbf{q}_0 = \frac{\pi}{c}(1, 0, 0)$ describes the antiferromagnetic order. Eq. (3.1) leads to a critical value of κ

$$\kappa_c = \frac{4}{2\zeta(3) - \eta(3)} \approx 2.66, \quad (3.3)$$

with $\zeta(n)$ and $\eta(n)$ defined in appendix A.

In the following we investigate the classical ground states and excitation spectra of the one-dimensional chain as a function of κ .

A. Exchange dominated region ($\kappa < \kappa_c$)

For pure exchange energy J , the classical ground state is the configuration where the spins are antiparallel, as described by the antiferromagnetic wave vector \mathbf{q}_0 . This state is continuously degenerate due to the rotational symmetry. The dipolar interaction breaks the rotational symmetry and favors the antiferromagnetic ground state, in which the spins lie in a plane perpendicular to the chain axis, as can be seen by the largest value of the dipole-dipole tensor ($A_{\mathbf{q}_0}^{33} = A_{\mathbf{q}_0}^{22} > A_{\mathbf{q}_0}^{11}$). However, rotation symmetry around the x -axis still exists (s.Fig. 1a).

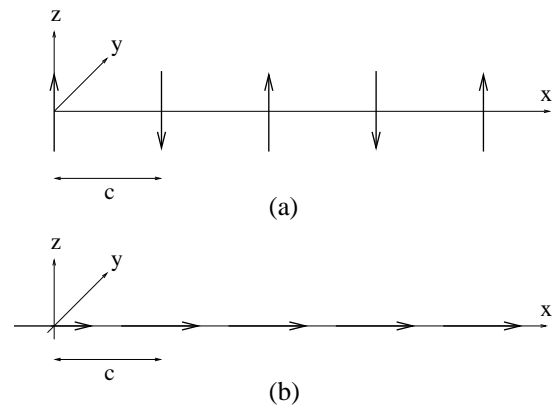


FIG. 1. a) Classical ground state of the dipolar, antiferromagnetic chain in the exchange dominated region ($\kappa < \kappa_c$). b) Ground state for the dipolar dominated region ($\kappa > \kappa_c$).

In the following calculations the primitive cell is the chemical cell which is half the magnetic unit cell. The antiferromagnetic modulation is taken into account via

$$\sigma_l = e^{i\mathbf{q}_0 \cdot \mathbf{x}_l} = \begin{cases} +1 & l \in \mathcal{L}_1 \\ -1 & l \in \mathcal{L}_2 \end{cases}, \quad \mathbf{q}_0 = \frac{\pi}{c}(1, 0, 0) \quad (3.4)$$

where \mathcal{L}_1 (\mathcal{L}_2) denotes the first (second) sublattice¹⁴. If we start from the classical ground state with the spins oriented along the $\pm z$ -axis and perform the Holstein-Primakoff transformation, we get the following Fourier transformed Hamiltonian

$$H = E_{cl} + \sum_{\mathbf{q}} A_{\mathbf{q}} a_{\mathbf{q}}^{\dagger} a_{\mathbf{q}} + \frac{1}{2} B_{\mathbf{q}} (a_{\mathbf{q}} a_{-\mathbf{q}} + a_{\mathbf{q}}^{\dagger} a_{-\mathbf{q}}^{\dagger}) \quad (3.5)$$

with the classical ground state energy

$$E_{cl} = -NS^2(J_{\mathbf{q}_0} + A_{\mathbf{q}_0}^{33}) \quad (3.6)$$

and the coefficients

$$\begin{aligned} A_{\mathbf{q}} &= S(2J_{\mathbf{q}_0} - J_{\mathbf{q}+\mathbf{q}_0} - J_{\mathbf{q}}) + S(2A_{\mathbf{q}_0}^{33} - A_{\mathbf{q}+\mathbf{q}_0}^{22} - A_{\mathbf{q}}^{11}) \\ B_{\mathbf{q}} &= S(J_{\mathbf{q}+\mathbf{q}_0} - J_{\mathbf{q}}) + S(A_{\mathbf{q}+\mathbf{q}_0}^{22} - A_{\mathbf{q}}^{11}). \end{aligned} \quad (3.7)$$

The Hamiltonian (3.5) is diagonalized by a Bogoliubov transformation¹⁵ and reads in terms of the new Bose creation and annihilation operators $b_{\mathbf{q}}^{\dagger}$ and $b_{\mathbf{q}}$

$$H = E_{cl} + \frac{1}{2} \sum_{\mathbf{q}} (E_{\mathbf{q}} - A_{\mathbf{q}}) + \sum_{\mathbf{q}} E_{\mathbf{q}} b_{\mathbf{q}}^{\dagger} b_{\mathbf{q}}. \quad (3.8)$$

The second term in Eq. (3.8) is a correction to the ground state energy due to quantum fluctuations, while the third term is the harmonic magnon Hamiltonian. The ground state energy

$$E(T=0) = E_{cl} + \frac{1}{2} \sum_{\mathbf{q}} (E_{\mathbf{q}} - A_{\mathbf{q}}) \quad (3.9)$$

is shown in Fig. 2 as a function of κ . The quantum fluctuations are strongest for pure exchange interaction¹⁶. The deviation of the ground state energy from the classical value

$$E(T=0) = E_{cl}(1 + 0.363/S), \quad (3.10)$$

is most significant in this case and decreases with increasing dipolar interaction, i.e. the dipolar interaction tends to stabilize the antiferromagnetic ground state.

The magnon dispersion relation reads

$$\begin{aligned} E_{\mathbf{q}} &= \sqrt{A_{\mathbf{q}}^2 - B_{\mathbf{q}}^2} \\ &= 2S \sqrt{(J_{\mathbf{q}_0} - J_{\mathbf{q}} + A_{\mathbf{q}_0}^{33} - A_{\mathbf{q}}^{11})} \\ &\quad \times \sqrt{(J_{\mathbf{q}_0} - J_{\mathbf{q}+\mathbf{q}_0} + A_{\mathbf{q}_0}^{33} - A_{\mathbf{q}+\mathbf{q}_0}^{22})}, \end{aligned} \quad (3.11)$$

which is shown in Fig. 3 for four values of κ . Because of the continuous degeneracy of the ground state (rotation around the x -axis) the Goldstone-mode at $\mathbf{q} = 0$ survives in the presence of the dipolar interaction, but the behavior for small wave vectors is modified. If we expand

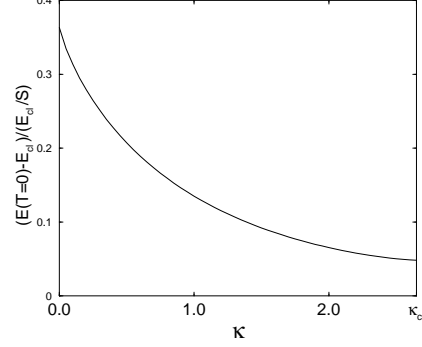


FIG. 2. Deviation of the ground state energy from the classical value due to quantum fluctuations for $\kappa < \kappa_c$. For $\kappa \geq \kappa_c$ there is no difference between the two energies, because the Hamiltonian is already diagonal after the HP-transformation (s. Eq. (3.20)).

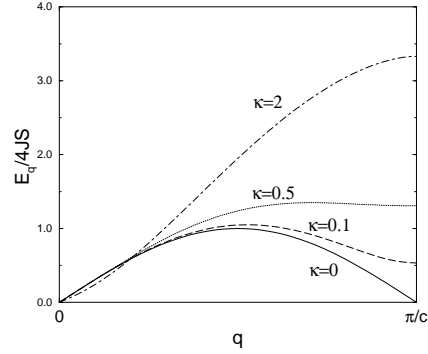


FIG. 3. Dispersion relation for different values of κ in the exchange dominated region ($\kappa \leq \kappa_c$).

the magnon spectrum around the center of the Brillouin zone, we get logarithmic corrections

$$\begin{aligned} E_{\mathbf{q}} / (4JS) &= \left\{ b_1 (qc)^2 - \frac{1}{4} \kappa \left(1 + \frac{1}{2} \kappa c_5 \right) (qc)^4 \log(qc) \right. \\ &\quad \left. + b_2 (qc)^4 + \mathcal{O}((qc)^6) \right\}^{1/2}, \end{aligned} \quad (3.12)$$

with q -independent constants c_5, b_1, b_2 (see Eq. A7, A14, A15 in Appendix A).

The order parameter, the staggered magnetization, is given by

$$N = g\mu_B \sum_l \sigma_l \langle \tilde{S}_l^z \rangle \quad (3.13)$$

with σ_l from Eq. (3.4). Inserting the Holstein-Primakoff transformation (2.3), we obtain

$$N = g\mu_B NS - N_0 - N_{th}(T) \quad (3.14)$$

with the zero-point contribution

$$N_0 = \frac{1}{2}g\mu_B \sum_{\mathbf{q}} \left(\frac{A_{\mathbf{q}}}{E_{\mathbf{q}}} - 1 \right) \quad (3.15)$$

and

$$N_{th}(T) = g\mu_B \sum_{\mathbf{q}} \frac{A_{\mathbf{q}}}{E_{\mathbf{q}}} n_{\mathbf{q}}, \quad (3.16)$$

from thermal excitations of spin waves. $n_{\mathbf{q}} = \frac{1}{e^{E_{\mathbf{q}}/kT} - 1}$ denotes the Bose-occupation number. Both quantum and thermal fluctuations reduce the order parameter. By use of the small wave vector expansion, Eq. (3.12), we see that the sum N_0 diverges for $\mathbf{q} \rightarrow 0$. Even though the dipolar interaction has the tendency to stabilize the antiferromagnetic order, it is nevertheless destroyed by quantum fluctuations even at $T = 0$, as found for the isotropic counterpart. There is yet another stability condition resulting from the requirement that the spin wave frequencies (Eq. (3.11)) be real which leads to

$$A_{\mathbf{q}} > 0 \quad (3.17)$$

$$A_{\mathbf{q}} > |B_{\mathbf{q}}| \quad (3.18)$$

for all wave vectors \mathbf{q} ¹⁷. We get a lower bound for the strength of the exchange energy from the first condition (Eq. (3.17)) at $\mathbf{q} = 0$

$$J_{\mathbf{q}_0} - J_0 + A_{\mathbf{q}_0}^{33} - A_0^{11} > 0. \quad (3.19)$$

For lower exchange energies the system changes to the dipolar dominated region.

B. Dipolar dominated region ($\kappa > \kappa_c$)

For pure dipolar interaction the classical ground state consists of two states, in which the spins are oriented ferromagnetically along the $\pm x$ -axis (Fig. 1b), because the largest eigenvalue of the dipolar tensor is A_0^{11} (s. Fig. 13), i.e. the dipolar interaction acts as an easy-axis anisotropy. If we start with this ground state and perform the HP-transformation we get

$$H = E_{cl} + \sum_{\mathbf{q}} E_{\mathbf{q}} a_{\mathbf{q}}^{\dagger} a_{\mathbf{q}}, \quad (3.20)$$

with the classical ground state energy

$$E_{cl} = -NS^2(J_0 + A_0^{11}) \quad (3.21)$$

and

$$E_{\mathbf{q}} = 2S(J_0 - J_{\mathbf{q}}) + 2S(A_0^{11} - A_{\mathbf{q}}^{33}). \quad (3.22)$$

Due to the broken rotation symmetry the spectrum has an energy gap at the zone center

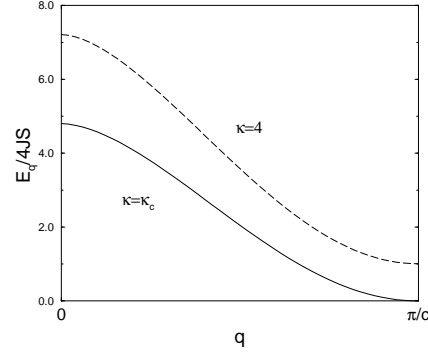


FIG. 4. Spin-wave dispersion relation of the dipolar, antiferromagnetic chain for $\kappa = \kappa_c = 2.66$ (solid) and $\kappa = 4$ (dashed).

$$E_0 = 2S(A_0^{11} - A_0^{33}).$$

The minimum of the dispersion relation is found at the zone edge (s. Fig. 4), which vanishes for $\kappa = \kappa_c$ and increases with increasing dipole strength.

In linear spin-wave theory the classical ground state and the quantum mechanical ground state coincide. The Hamiltonian (3.20) is diagonalized by the HP-transformation, and there are no corrections for quantum fluctuations¹⁸ at $T = 0$, i.e. the ground state has long-range order. The order parameter is the magnetization in x -direction:

$$M^x = g\mu_B \sum_l \langle S_l^x \rangle = g\mu_B NS - M_{th}(T) \quad (3.23)$$

with

$$M_{th}(T) = g\mu_B \sum_{\mathbf{q}} \frac{1}{e^{E_{\mathbf{q}}/k_B T} - 1}. \quad (3.24)$$

For $\kappa > \kappa_c$ the spin-wave spectrum has gaps at $\mathbf{q} = 0$ and $\mathbf{q} = \mathbf{q}_0$ (Eq. (3.22)). Thus, the sum in Eq. (3.24) is finite for finite temperatures and from point of view of the linear spin-wave theory long-range order should be possible. However, as was shown by Dyson¹⁹, kink-like thermal excitations destroy the long-range order in ferromagnetic Ising systems with interactions decreasing like $J(r) \propto \frac{1}{r^\alpha}$ for $\alpha > 2$. Thus, we expect that for a Heisenberg system with dipole-dipole interaction these nonlinear excitations will ultimately destroy the long-range order as well.

Stability of the ground state requires that the spectrum is positive, $E_{\mathbf{q}} > 0$. For decreasing dipole energy the instability of the spectrum sets in at \mathbf{q}_0 , from which we recover the stability condition Eq. (3.1)

$$J_{\mathbf{q}_0} - J_0 + A_{\mathbf{q}_0}^{33} - A_0^{11} < 0. \quad (3.25)$$

The soft mode at \mathbf{q}_0 for $\kappa = \kappa_c$ indicates the phase transition to the antiferromagnetic phase (exchange-dominated region).

Consequently at $T = 0$ there is long-range order (LRO) in the dipolar dominated region, in contrast to the exchange dominated region. However, for finite temperatures no LRO exists at all due to nonlinear excitations, namely domain walls.

IV. MAGNETIC PHASE DIAGRAM

In this section we determine the magnetic phase diagram of the dipolar antiferromagnetic chain for both the dipolar dominated and the exchange dominated region. We study homogeneous magnetic fields along and perpendicular to the chain axis (x -direction). The results are presented in terms of the parameter κ (Eq. (2.4)) and the dimensionless field $h = \frac{g\mu_B H_0}{JS}$. The spin orientations are determined from the classical ground state energy within a two-sublattice model.

A. Field in chain direction

First we study the case of a magnetic field along the chain axis. In the dipolar region ($\kappa > \kappa_c$) the field is parallel to the spins, and thus no reorientation takes place.

In the exchange dominated region ($\kappa < \kappa_c$) the spins are oriented perpendicular to the x -axis and any infinitesimal field along the axis will lead to a reorientation of the spins in order to gain energy from the Zeeman term (Eq. (2.1)). In a two-sublattice model (the spins of the sublattice $\mathcal{L}_1(\mathcal{L}_2)$ enclose an angle $\varphi_1(\varphi_2)$ with the y - z -plane (see Fig. 5)) we can calculate the classical ground state energy. For spins lying in the xz -plane we get

$$E_{cl} = -\frac{NS^2}{4} \left[(J_0 + A_0^{11})(\sin \varphi_1 + \sin \varphi_2)^2 + (J_{\mathbf{q}_0} + A_{\mathbf{q}_0}^{11})(\sin \varphi_1 - \sin \varphi_2)^2 + (J_0 + A_0^{33})(\cos \varphi_1 - \cos \varphi_2)^2 + (J_{\mathbf{q}_0} + A_{\mathbf{q}_0}^{33})(\cos \varphi_1 + \cos \varphi_2)^2 \right] - \frac{1}{2}g\mu_B H_0^x NS(\sin \varphi_1 + \sin \varphi_2). \quad (4.1)$$

Minimization with respect to φ_1 and φ_2 yields $\varphi_1 = \varphi_2 = \varphi$, i.e. a usual spin-flop phase. From the minimum one determines the relation between the angle φ and the magnetic field:

$$\sin \varphi = \frac{g\mu_B H_0^x}{2S(J_{\mathbf{q}_0} - J_0 + A_{\mathbf{q}_0}^{33} - A_0^{11})}. \quad (4.2)$$

Thus the spins become progressively aligned along the field as the field increases. There is a continuous transition from this spin-flop phase to the paramagnetic phase for $\varphi = 90^\circ$. The transition occurs at

$$h_c^x(\kappa) = 8 + \kappa(2\eta(3) - 4\zeta(3)) \quad \text{for } \kappa < \kappa_c. \quad (4.3)$$

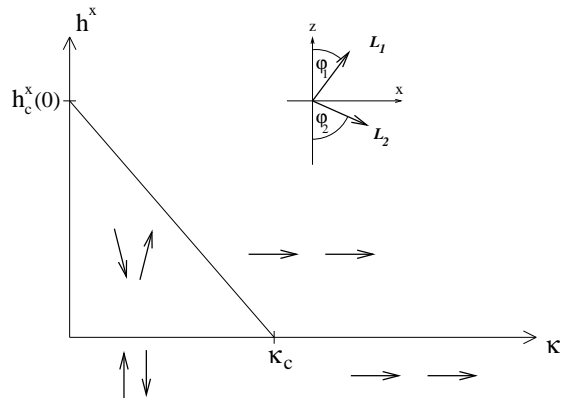


FIG. 5. Magnetic phase diagram of the dipolar, antiferromagnetic chain with a field applied in chain direction. The spin arrangements below the x -axis indicate the phases for vanishing field. In the insert the configuration of the spins in a two-sublattice model is shown.

The complete phase diagram is shown in Fig. 5. The HP-transformed Hamiltonian in the spin-flop phase has the form of Eq. (3.5) with coefficients

$$A_{\mathbf{q}} = S(2J_{\mathbf{q}_0} - J_{\mathbf{q}+\mathbf{q}_0} - J_{\mathbf{q}} + 2A_{\mathbf{q}_0}^{33} - A_{\mathbf{q}+\mathbf{q}_0}^{22} - A_{\mathbf{q}}^{11}) + S \sin^2 \varphi (J_{\mathbf{q}} - J_{\mathbf{q}+\mathbf{q}_0} + A_{\mathbf{q}}^{11} - A_{\mathbf{q}+\mathbf{q}_0}^{33}) \\ B_{\mathbf{q}} = S(J_{\mathbf{q}+\mathbf{q}_0} - J_{\mathbf{q}} + A_{\mathbf{q}+\mathbf{q}_0}^{22} - A_{\mathbf{q}}^{11}) + S \sin^2 \varphi (J_{\mathbf{q}} - J_{\mathbf{q}+\mathbf{q}_0} + A_{\mathbf{q}}^{11} - A_{\mathbf{q}+\mathbf{q}_0}^{33}), \quad (4.4)$$

where φ is related to the field by Eq. (4.2). The dispersion relation is shown in Fig. 6 for two values of the field.

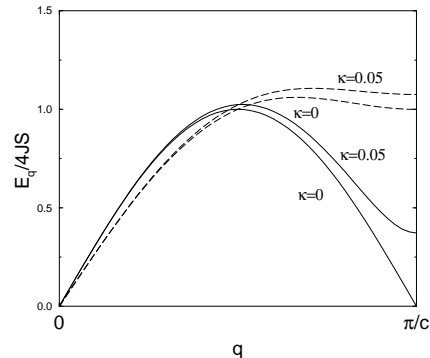


FIG. 6. Dispersion relation for the linear chain in the spin-flop phase for two values of κ ; solid lines for vanishing field and dashed lines for $\sin \varphi = 0.5$ (Eq. (4.2)).

The Goldstone-mode at $\mathbf{q} = 0$ remains for finite dipolar energy because the system is still invariant for rotations around the x -axis.

The magnetization in the spin-flop phase can be calculated from the free energy F

$$\mathbf{M} = -\frac{\partial F}{\partial \mathbf{H}_0}. \quad (4.5)$$

The free energy F is related to the partition function Z by

$$F = -kT \log Z \quad \text{with} \quad Z = \text{Spe}^{-\beta H} \quad \text{and} \quad \beta = \frac{1}{k_B T},$$

i.e. for the Hamiltonian (3.8)

$$F = E_{cl} + \frac{1}{2} \sum_{\mathbf{q}} (E_{\mathbf{q}} - A_{\mathbf{q}}) + k_B T \sum_{\mathbf{q}} \log(1 - e^{-\beta E_{\mathbf{q}}}). \quad (4.6)$$

Inserting Eq. (4.6) into (4.5) yields for the magnetization

$$\mathbf{M} = \mathbf{M}_{cl} - \mathbf{M}_0 - \mathbf{M}_{th}(T), \quad (4.7)$$

which consists of a classical part

$$\mathbf{M}_{cl} = -\frac{\partial E_{cl}}{\partial \mathbf{H}_0}, \quad (4.8)$$

a part arising from quantum fluctuations ($T = 0$)

$$\mathbf{M}_0 = \frac{1}{2} \sum_{\mathbf{q}} \left\{ \frac{1}{E_{\mathbf{q}}} \left(B_{\mathbf{q}} \frac{\partial B_{\mathbf{q}}}{\partial \mathbf{H}_0} - A_{\mathbf{q}} \frac{\partial A_{\mathbf{q}}}{\partial \mathbf{H}_0} \right) + \frac{\partial A_{\mathbf{q}}}{\partial \mathbf{H}_0} \right\} \quad (4.9)$$

and a part arising from thermal fluctuations

$$\mathbf{M}_{th}(T) = \sum_{\mathbf{q}} \frac{1}{e^{\beta E_{\mathbf{q}}} - 1} \frac{1}{E_{\mathbf{q}}} \left(B_{\mathbf{q}} \frac{\partial B_{\mathbf{q}}}{\partial \mathbf{H}_0} - A_{\mathbf{q}} \frac{\partial A_{\mathbf{q}}}{\partial \mathbf{H}_0} \right). \quad (4.10)$$

The classical magnetization is reduced by quantum and thermal fluctuations. For the spin-flop phase the classical magnetization can be obtained by inserting the expression for the classical ground state energy (Eq. (4.1)) in Eq. (4.8). We get

$$M_{cl}^x = g\mu_B N S \sin \varphi, \quad (4.11)$$

where $\sin \varphi$ is given by Eq. (4.2). The contributions of quantum and thermal fluctuations will be taken into account numerically when we compare our results with experiments (s. section IV).

Now we turn to the staggered magnetization in the z -direction

$$N_z = g\mu_B \sum_l \sigma_l \langle S_l^z \rangle, \quad (4.12)$$

which leads to

$$N_z = g\mu_B \cos \varphi \left(NS - \frac{1}{2} \sum_{\mathbf{q}} \left(\frac{A_{\mathbf{q}}}{E_{\mathbf{q}}} - 1 \right) - \sum_{\mathbf{q}} \frac{A_{\mathbf{q}}}{E_{\mathbf{q}}} n_{\mathbf{q}} \right). \quad (4.13)$$

The second and third term in (4.13) are divergent due to the Goldstone-mode. Thus, no antiferromagnetic long-range order is possible in this case, only a finite magnetization.

B. Field perpendicular to the chain direction

1. Exchange-dominated region ($\kappa < \kappa_c$)

A field perpendicular to the chain leads to a spin-flop transition; for infinitesimal fields the spins lie in the yz -plane and perpendicular to the applied field. With increasing field the spins become progressively aligned in field direction. In the following calculations the field is applied in the y -direction so that for infinitesimal field the spins are oriented in the $\pm z$ -direction. Again, we study the classical ground state energy of a general two-

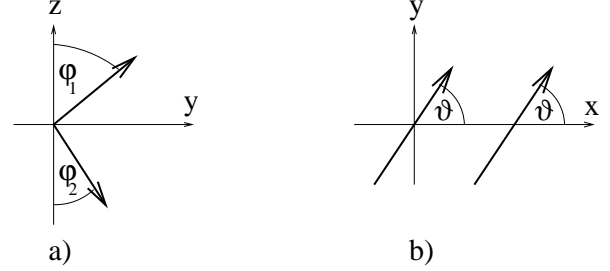


FIG. 7. Configuration of the spins for a field applied perpendicular to the chain axis; a) for the exchange-dominated region, $\kappa < \kappa_c$, b) for $\kappa > \kappa_c$.

sublattice system, for which the usual spin-flop phase turns out to be stable. The equilibrium condition leads to

$$\sin \varphi = \frac{g\mu_B H_0^y}{2S(J_{\mathbf{q}_0} - J_0 + A_{\mathbf{q}_0}^{33} - A_0^{22})}, \quad (4.14)$$

in analogy to Eq. (4.2) for fields along the chain axis, which differs only in the dependence on the dipole interaction. The transition between the spin-flop phase and the paramagnetic phase occurs at (see Fig. 10)

$$h_c^y(\kappa) = 8 + \kappa(2\eta(3) + 2\zeta(3)) \quad \text{for} \quad \kappa < \kappa_c. \quad (4.15)$$

The coefficients of the Hamiltonian, Eq. (3.5), in the spin-flop phase are in linear spin-wave theory

$$\begin{aligned} A_{\mathbf{q}} &= S(2J_{\mathbf{q}_0} - J_{\mathbf{q}+\mathbf{q}_0} - J_{\mathbf{q}} + 2A_{\mathbf{q}_0}^{33} - A_{\mathbf{q}+\mathbf{q}_0}^{22} - A_{\mathbf{q}}^{11}) \\ &\quad + S \sin^2 \varphi (J_{\mathbf{q}+\mathbf{q}_0} - J_{\mathbf{q}} + A_{\mathbf{q}+\mathbf{q}_0}^{22} - A_{\mathbf{q}}^{33}), \\ B_{\mathbf{q}} &= S(J_{\mathbf{q}+\mathbf{q}_0} - J_{\mathbf{q}} + A_{\mathbf{q}+\mathbf{q}_0}^{22} - A_{\mathbf{q}}^{11}) \\ &\quad + S \sin^2 \varphi (J_{\mathbf{q}} - J_{\mathbf{q}+\mathbf{q}_0} + A_{\mathbf{q}}^{33} - A_{\mathbf{q}+\mathbf{q}_0}^{22}). \end{aligned} \quad (4.16)$$

For finite κ rotational symmetry is lost for the spin configuration of Fig. 7a and thus no Goldstone-mode is present in the dispersion relation of Fig. 8 showing the spectrum for two different values of κ and H_0^y . The magnetization in the y -direction is obtained from the free energy (see Eq. (4.5)) and is of the same form as Eqn. (4.7)-(4.11) with different canting angle $\sin \varphi$ (Eq. (4.14)) and different coefficients $A_{\mathbf{q}}$ and $B_{\mathbf{q}}$ (Eq. (4.16)).

$$h_c^y(\kappa) = 6\zeta(3)\kappa \quad \text{for } \kappa > \kappa_c. \quad (4.20)$$

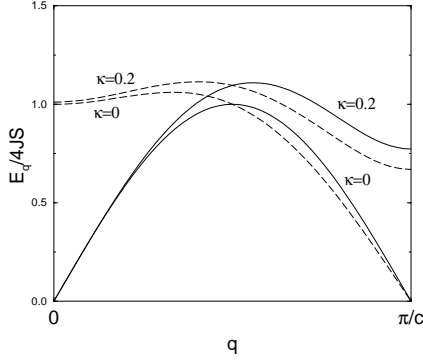


FIG. 8. Dispersion relation in the spin-flop phase for different magnetic fields applied perpendicular to the chain direction and different strengths of the dipolar interaction. The solid lines are without field and the dashed lines are for $\sin \varphi = 0.5$ (Eq. (4.2)).

Now the staggered magnetization in z -direction, which in analogy to Eqs. (4.12)-(4.13) is given by

$$N_z = g\mu_B \cos \varphi \left(NS - \frac{1}{2} \sum_{\mathbf{q}} \left(\frac{A_{\mathbf{q}}}{E_{\mathbf{q}}} - 1 \right) - \sum_{\mathbf{q}} \frac{A_{\mathbf{q}}}{E_{\mathbf{q}}} n_{\mathbf{q}} \right), \quad (4.17)$$

is finite, because of the energy gap in $E_{\mathbf{q}}$ (s. Fig. 8). However, we believe that due to nonlinear kink-like excitations again no long-range order is possible for finite temperatures.

If the field is applied in chain direction a Goldstone-mode remains (s. Fig. 6) and hence the expression for the staggered magnetization N_z diverges (Eq. (4.13)).

2. Dipole dominated region ($\kappa > \kappa_c$)

In this region the spins keep the ferromagnetic orientation but with a canting angle ϑ (intermediate phase) with respect to the magnetic field (s. Fig. 7b). The classical ground state energy is given by

$$E_{cl} = -NS^2 [(J_0 + A_0^{22}) \sin^2 \vartheta + (J_0 + A_0^{11}) \cos^2 \vartheta] - g\mu_B H_0^y NS \sin \vartheta, \quad (4.18)$$

the minimization of which gives the following relation between the canting angle ϑ and the applied field H_0^y :

$$\sin \vartheta = \frac{g\mu_B H_0^y}{2S(A_0^{11} - A_0^{22})}. \quad (4.19)$$

Note that this angle depends only on the dipole strength but not on the exchange energy due to the isotropy of $J_{\mathbf{q}}$. The transition to the paramagnetic phase, in which all spins orient along the magnetic field, occurs at

The coefficients in the Fourier transformed Hamiltonian for finite canting angle ϑ are given by

$$\begin{aligned} A_{\mathbf{q}} &= 2S(J_0 - J_{\mathbf{q}}) + 2S(A_0^{11} - A_{\mathbf{q}}^{22}) \\ &\quad + S \sin^2 \vartheta (A_{\mathbf{q}}^{22} - A_{\mathbf{q}}^{11}) \\ B_{\mathbf{q}} &= S \sin^2 \vartheta (A_{\mathbf{q}}^{22} - A_{\mathbf{q}}^{11}). \end{aligned} \quad (4.21)$$

The spectrum is shown for three values of the field in Fig. 9. For decreasing field the energy gap $E_{\mathbf{q}_0}$ decreases until it vanishes at the transition point. Now we investigate

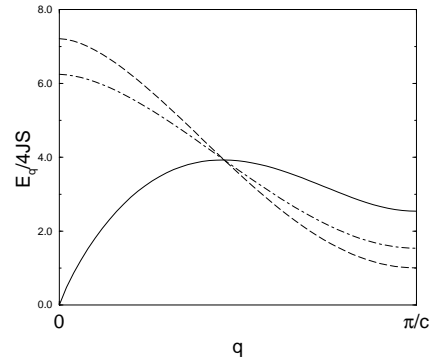


FIG. 9. Dispersion relation for the dipole dominated region with a field perpendicular to the chain direction and $\kappa = 4$; dashed: $\sin \vartheta = 0$, dot-dashed: $\sin \vartheta = 0.5$ and solid: $\sin \vartheta = 1$.

the transition from the spin-flop phase to the intermediate phase as a function of κ . Comparison of the classical ground state energy of the two phases shows that the transition line is independent of the applied field H_0^y (if $H_0^y < H_c^y$), which explains the vertical line at $\kappa = \kappa_c$ between the spin-flop phase and the intermediate phase in the phase diagram of Fig. 10. For $\kappa < \kappa_c$ the spin-flop phase has lower energy and is thus the stable phase, for $\kappa > \kappa_c$ the intermediate phase has lower energy. At $\kappa = \kappa_c$ and $h = h_c$ the energies of the spin-flop phase, the intermediate phase and the paramagnetic phase are the same.

V. COMPARISON WITH EXPERIMENT

In this section we compare our theoretical results with measurements on quasi one-dimensional antiferromagnets in the hexagonal ABX_3 structure. Due to different exchange mechanisms the intrachain interaction is about three orders of magnitude larger than the interchain interaction, thus that these materials behave in a quasi one-dimensional manner. The most promising substances are the manganese compounds, because Mn^{2+} ions have spin $S = 5/2$ and vanishing orbital momentum. Thus, the main contribution to the anisotropy should be the

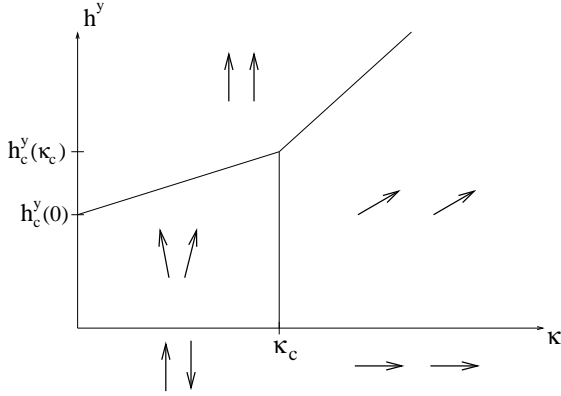


FIG. 10. Magnetic phase diagram of the dipolar, antiferromagnetic chain with a field perpendicular to the chain axis. The configurations below the x -axis correspond to vanishing field.

dipole-dipole interaction. The field-dependent magnetization has been measured for RbMnBr_3 (Fig. 11 dashed lines)⁸. In this material the spins are forced to orient within the hexagonal plane, perpendicular to the chain-axis. This planar anisotropy can be fully explained by the dipole-dipole interaction, which leads in the exchange-dominated region to just such an orientation (see section II). Magnetization experiments show an anisotropy: the magnetization for magnetic fields along the spin-chain axis is about 5 to 10% larger than for fields perpendicular to it. Part of this anisotropy can be understood qualitatively even for classical spins by the dipolar anisotropy, which leads to different dependences of the angle φ of the spins on the magnetic field (Eqs. (4.2) and (4.14)). The classical contribution to the magnetization is larger for parallel than perpendicular field, since the dipole interaction favors ferromagnetic orientation in chain direction. For a quantitative comparison we need the values of the exchange energy J and the lattice constant c which are given for RbMnBr_3 by²⁰

$$J = 9.56K, \quad c = 3.26\text{\AA}.$$

Here the exchange energy was determined by a fit of the spin-wave curves with the spin-wave spectrum calculated from a Hamiltonian in which the anisotropy is described by a single-ion term. For this Hamiltonian there exists a renormalization calculation²¹, which shows, that the classical value of the exchange energy has to be renormalized due to magnon-magnon interactions. The resulting value of J is

$$J = 8.93K.$$

This corresponds to $\kappa = 8.07 \cdot 10^{-3}$, which is deep in the exchange dominated region of our theory. With this constant we calculate the classical contributions to the magnetization (see Eq. (4.11)) in the spin-flop phase shown in Fig. 11 as the upper and lower thin solid

lines for fields along and perpendicular to the chain-axis. The dashed lines represent the experimental values. The transition to the paramagnetic phase takes place at $H_c \approx 130T$ and cannot be seen here. For perpendicular fields lower than $H \approx 3.9T$ the three-dimensional ordering becomes important: the system changes to a complicated six-sublattice structure²² for which our one-dimensional model is inappropriate. According to Fig. 11, the classical magnetization is larger than the experimental and the splitting for the two directions is almost invisible. However, in one dimension the quantum fluctuations are strong and must be taken into account. Numerical evaluation of the magnetization for longitudinal and perpendicular field direction (Eq. (4.7)), including the zero-point contributions ($T = 0$), yields the thick solid lines in Fig. 11. In fact, the quantum fluctuations lead to a pronounced reduction of the magnetization and increase the splitting, but as to be expected, are somewhat overestimated in the pure one-dimensional model. The contribution of thermal fluctuations to the magnetization (Eq. (4.10)) is negligible for temperatures as low as in the experiment ($T = 1.7K$). This is in contrast to the work of Santini et al.¹⁰, who claim that the classical thermal fluctuations are the relevant contribution and totally neglect the quantum fluctuations. Abanov and Petrenko⁸ also studied the one-dimensional spin-chain, but with a single-ion anisotropy favoring orientation perpendicular to the chain instead of the dipolar interaction. Inserting the fitted value for this anisotropy they get a larger fluctuation contribution than in our theory. Furthermore, the classical contribution shows the opposite anisotropy, i.e. the magnetization for a field along the chain-axis is lower than for a perpendicular field.

In summary, we can explain the anisotropy measured in RbMnBr_3 qualitatively by a one-dimensional, dipolar Heisenberg model. We expect that by taking into account the full three-dimensional structure with interactions between different chains the quantitative agreement could be improved because the contribution of quantum fluctuations is reduced in higher dimensions. Our prediction for the spin wave dispersion relation of RbMnBr_3 (Eq. (3.11)) is shown in the magnetic Brillouin zone in Fig. 12. Here we set the exchange interaction J to $9.56K$. The resulting gap of the upper dispersion branch at $\mathbf{q} = 0$ equals $14.16K$.

VI. SUMMARY

We have considered the one-dimensional, isotropic Heisenberg antiferromagnet with dipole-dipole interaction in the complete parameter region. We showed that there exists an exchange dominated phase for $\kappa < \kappa_c$, where the spins orient antiferromagnetically, perpendicular to the chain axis, i.e. the dipole-dipole interaction gives rise to a planar anisotropy. For $\kappa > \kappa_c$, the dipole-dominated phase, the ground state is ferromagnetic along

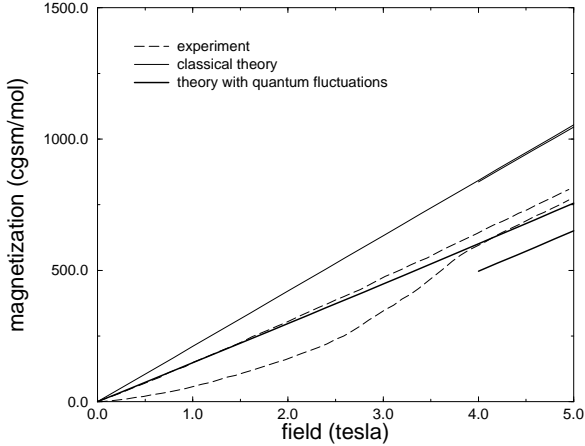


FIG. 11. Magnetization curves for RbMnBr_3 ⁸: The dashed lines show the experimental measurements at $T = 1.7\text{K}$. The thin lines show the classical results of our theory, i.e. without quantum fluctuations. The thick lines show the results taking into consideration quantum fluctuations. For each pair of curves the upper one refers to field parallel and the lower one to field perpendicular to the chain.

the chain axis, i.e. the dipole-dipole interaction acts like an easy-axis anisotropy. Because of the broken rotation symmetry the dipole-dominated region shows long-range order for $T = 0$. In the exchange-dominated region there is still a Goldstone-mode due to the rotation symmetry around the chain axis. Although the linear small \mathbf{q} behavior of the acoustic magnon mode is modified by the dipole energy (Eq. (3.12)), there is no long-range order neither for finite nor for zero temperature.

The magnetic phase diagram for fields along and perpendicular to the chain in both the dipole and the exchange dominated regions has been determined and the predicted magnetization has been compared with experiments on RbMnBr_3 , a quasi one-dimensional, planar antiferromagnet. The experimental anisotropy can be explained qualitatively by the one-dimensional, dipolar model, the quantitative agreement could be improved by a more elaborate, three-dimensional calculation.

ACKNOWLEDGMENTS

This work has been supported by the BMBF under contract number 03-SC4TUM. One of us (M.H.) has benefited from a scholarship of the Studienstiftung des Deutschen Volkes. The work of C.P. has been supported by the Deutsche Forschungsgemeinschaft (DFG) under the contract no. PI 337/1-1.

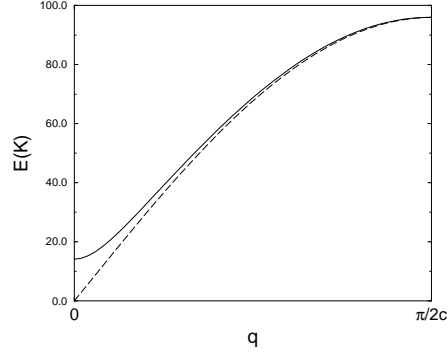


FIG. 12. The two branches of the dispersion relation for RbMnBr_3 in the magnetic Brillouin zone with dipolar interaction ($\kappa = 8.072 \cdot 10^{-3}$, $J = 9.56 \text{ K}$).

APPENDIX A: DIPOLAR SUMS

The dipolar sums can be evaluated in Fourier space by the Ewald method²³. The sum in Fourier space is divided into a sum over the direct lattice and a sum over the indirect lattice, so that both sums converge quickly. The dipolar tensor in one dimension finally reads (all values of the dipolar tensor are measured in units of $\frac{(g\mu_B)^2}{2c^3}$)

$$A_{\mathbf{q}}^{\alpha\beta} = \begin{cases} \frac{4}{3}\pi - 2\pi \sum_l' e^{i\mathbf{q}\cdot\mathbf{x}_l} \varphi_{\frac{1}{2}}\left(\frac{\pi}{c^2}|\mathbf{x}_l|^2\right) - 2\pi \sum_r \varphi_{-2}\left(\frac{c^2}{4\pi}|\mathbf{q} + \mathbf{G}_r|^2\right) & \alpha = \beta \notin \mathbf{x}_l \\ \frac{4}{3}\pi\delta_{\alpha\beta} - 2\pi\delta_{\alpha\beta} \sum_l' e^{i\mathbf{q}\cdot\mathbf{x}_l} \varphi_{\frac{1}{2}}\left(\frac{\pi}{c^2}|\mathbf{x}_l|^2\right) + 4\frac{\pi^2}{c^2} \sum_l' e^{i\mathbf{q}\cdot\mathbf{x}_l} x_l^\alpha x_l^\beta \varphi_{\frac{3}{2}}\left(\frac{\pi}{c^2}|\mathbf{x}_l|^2\right) - c^2 \sum_r (\mathbf{q} + \mathbf{G}_r)_\alpha (\mathbf{q} + \mathbf{G}_r)_\beta \times \varphi_{-1}\left(\frac{c^2}{4\pi}|\mathbf{q} + \mathbf{G}_r|^2\right) & \alpha, \beta \in \mathbf{x}_l, \end{cases} \quad (\text{A1})$$

where $\mathbf{x}_l = lc(1, 0, 0)$ and $\mathbf{G}_r = \frac{2\pi}{c}r(1, 0, 0)$. The prime at the l -summations denotes $l \neq 0$. We have to distinguish between components with spins lying in the chain direction ($\alpha, \beta \in \mathbf{x}_l$) and those perpendicular to it ($\alpha, \beta \notin \mathbf{x}_l$). The off-diagonal components are identical zero due to the inversion symmetry. The dipolar sums are shown in Fig. (13) as a function of \mathbf{q} . In Eq. (A1) we have introduced the Misra functions

$$\varphi_n(x) = \int_1^\infty dt t^n e^{-xt}. \quad (\text{A2})$$

The asymptotic behavior of the Misra functions for small arguments x is

$$\varphi_{-1}(x) \approx (-\gamma - \log x) + x - \frac{1}{4}x^2 + \mathcal{O}(x^3) \quad (\text{A3})$$

and

$$\varphi_{-2}(x) \approx 1 + (-1 + \gamma + \log x)x - \frac{1}{2}x^2 + \mathcal{O}(x^3), \quad (\text{A4})$$

where $\gamma \approx 0.5772$ is Euler's constant. The expansion of the dipolar tensor needed in Eq. (3.12) reads

$$A_{\mathbf{q}}^{11} = c_1 - c_2(qc)^2 + (qc)^2 \log\left(\frac{(qc)^2}{4\pi}\right) + c_3(qc)^4 + \mathcal{O}\left((qc)^6\right) \quad (\text{A5})$$

$$A_{\mathbf{q}+\mathbf{q}_0}^{22} = A_{\mathbf{q}+\mathbf{q}_0}^{33} = c_4 - c_5(qc)^2 + c_6(qc)^4 + \mathcal{O}\left((qc)^6\right), \quad (\text{A6})$$

where the constants c_1, c_4 are given analytically in Eq. (A8) and (A10), while the others are computed numerically as

$$c_2 \approx 0.666, \quad c_3 \approx 0.066, \quad c_5 \approx 0.693 \quad \text{and} \quad c_6 \approx 0.021. \quad (\text{A7})$$

The dipolar tensor can be evaluated exactly for some configurations. For the ferromagnetic order of the spins along the x -axis one gets

$$A_0^{11} = 4 \sum_{l>0} \frac{1}{l^3} = 4\zeta(3) = c_1 \approx 4.808, \quad (\text{A8})$$

where $\zeta(n)$ is the Riemann zeta function²⁴

$$\zeta(n) = \sum_{l=1}^{\infty} l^{-n}. \quad (\text{A9})$$

The antiferromagnetic order of the spins along the z -axis yields

$$A_{\mathbf{q}_0}^{33} = 2 \sum_{l>0} \frac{(-1)^{l-1}}{l^3} = 2\eta(3) = c_4 \approx 1.803 \quad (\text{A10})$$

where the eta function $\eta(n)$ is defined by²⁴

$$\eta(n) = \sum_{l=1}^{\infty} (-1)^{l-1} l^{-n}. \quad (\text{A11})$$

Other exact values are

$$A_0^{33} = -2\zeta(3) \quad \text{and} \quad A_{\mathbf{q}_0}^{11} = -4\eta(3). \quad (\text{A12})$$

These values corroborate the sums in Eq. (A1). One can show that for the dipolar tensor components of the linear chain the relation

$$A_{\mathbf{q}}^{11} + A_{\mathbf{q}}^{22} + A_{\mathbf{q}}^{33} = A_{\mathbf{q}}^{11} + 2A_{\mathbf{q}}^{22} = 0 \quad (\text{A13})$$

is valid.

The constants in Eq.(3.12) are given by

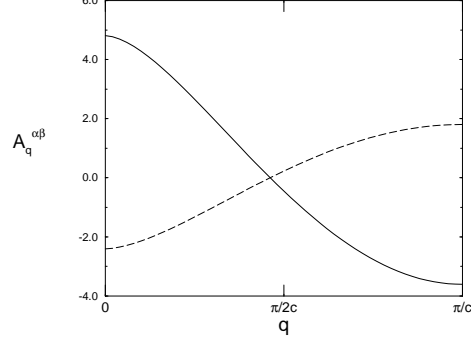


FIG. 13. Dipole sums $A_{\mathbf{q}}^{\alpha\beta}$ in Fourier space given in units of $\frac{(g\mu_B)^2}{2c^3}$. The solid line denotes $A_{\mathbf{q}}^{11}$ and the dashed $A_{\mathbf{q}}^{22} = A_{\mathbf{q}}^{33}$. All non-diagonal components vanish.

$$b_1 = \frac{1}{16} \left(8 - \kappa(4\zeta(3) - 2\eta(3)) \right) (2 + \kappa c_5) \quad (\text{A14})$$

$$b_2 = -\frac{1}{3} + \kappa \left(\frac{1}{96} (4\zeta(3) - 2\eta(3)) + \frac{1}{8} (c_2 - c_5) - \frac{1}{2} c_6 + \frac{1}{16} \kappa c_2 c_5 + \frac{1}{16} \kappa c_6 (4\zeta(3) - 2\eta(3)) + \frac{1}{8} \log(4\pi) + \frac{1}{16} \kappa c_5 \log(4\pi) \right). \quad (\text{A15})$$

-
- ¹ P.C. Hohenberg, Phys. Rev. **158**, 383 (1967).
 - ² N.D. Mermin, H. Wagner, Phys. Rev. Lett. **17**, 1133 (1966).
 - ³ S.V. Maleev, Zh.Eksp. Teor.Fiz. **70**, 2375 (1976) [Sov.Phys. JETP **43**, 1240 (1976)].
 - ⁴ C. Pich and F. Schwabl, Phys. Rev. **B 47**, 7957 (1993), Ibid. **B 49**, 413 (1994).
 - ⁵ C. Pich and F. Schwabl, J. Magn. Magn. Mat. **140-144**, 1709 (1995), Ibid. **148**, 30 (1995).
 - ⁶ F.D.M. Haldane, Phys. Rev. Lett. **50**, 1153 (1983).
 - ⁷ M. Steiner, M.J. Mikeska, Adv. Phys. **40**, 191 (1991).
 - ⁸ A.G. Abanov and O.A. Petrenko, Phys. Rev. **B 50**, 6271 (1994).
 - ⁹ H. Shiba, N. Suzuki, J. Phys. Soc. Jpn. **51**, 3488 (1982).
 - ¹⁰ P. Santini, Z. Domanski, J. Dong and P. Erdős, Phys. Rev. **B 54**, 6327 (1996).
 - ¹¹ M. Steiner, In S.W. Lovesey, U. Balucani, F. Borsa, and V. Tognetti, editors, *Magnetic Excitations and Fluctuations*, (Springer, Berlin Heidelberg New York Tokyo, 1984).
 - ¹² T. Holstein and H. Primakoff, Phys. Rev. **58**, 1098 (1940).
 - ¹³ P.P. Ewald, Ann. Phys. (Leipz.) **64**, 253 (1921).
 - ¹⁴ J.M. Ziman, *Principles of the Theory of Solids*, (Cambridge University Press, Cambridge, England, 1969), p. 317ff.

- ¹⁵ A.I. Akhiezer, V.G. Bar'yakhtar and S.V. Peletminskii, *Spin waves*, (North Holland Publishing Company, 1968).
- ¹⁶ P.W. Anderson, Phys. Rev. **86**, 694 (1952).
- ¹⁷ M.H. Cohen, F. Keffer, Phys. Rev. **99**, 1135 (1955).
- ¹⁸ It can be shown that the ferromagnetic orientation is the exact ground state of the dipolar chain, C. Pich, to be published.
- ¹⁹ F.J. Dyson, Commun. math. Phys. **12**, 91-107 (1969).
- ²⁰ L. Heller, M.F. Collins, Y.S. Yang and B. Collier, Phys. Rev. **B 49**, 1104 (1994).
- ²¹ D.V. Khveshchenko and A.V. Chubukov, Zh.Eksp. Teor. Fiz. **93**, 1904 (1987) [Sov.Phys. JETP **66**, 1088 (1987)].
- ²² A.V. Chubukov, J. Phys. C: Sol.St.Phys. **21**, 441 (1988).
- ²³ L. Bonsall and A.A. Maradudin, Phys. Rev. **B 15**, 1959 (1977).
- ²⁴ M. Abramowitz, *Pocketbook of Mathematical Functions*, Verlag Harri Deutsch, p.362, (1984).